Proceedings of the International Society for Magnetic Resonance in Medicine 2016; **24**: 4290.

Assessment of geometric distortion in six clinical scanners using a 3D-Printed Grid Phantom

Maysam M Jafar[1], Christopher E Dean[1], Malcolm J Birch[1], and Marc E Miquel[1]

[1]*Clinical Physics, Barts Health NHS Trust, City of London, United Kingdom*

Synopsis

Major hardware-related geometric distortions in MRI arise from gradient field non-linearity and static field inhomogeneity. For an accurate mapping of geometrical distortion in 3D, the number of control points must be sufficiently large to provide a comprehensive mapping of the spatial variation of distortion and the positional accuracy of these control points must be ensured. In this study, the spatial accuracy of coordinates in 3D space is assessed across six clinical MRI scanners at both 1.5T and 3T field strengths using a previously reported 3D-printed grid phantom. This is a cost-effective approach to determine the spatial accuracy of control points.

Purpose

Magnetic resonance imaging (MRI) offers superior soft-tissue contrast compared with computed tomography (CT) but suffers from inherent geometric distortions. Major hardware-related geometric distortions arise from gradient field non-linearity and static field inhomogeneity. Geometric distortions occurring due to non-linearity in the gradient fields outweigh those occurring due to static field inhomogeneity as modern superconducting MRI systems are equipped with active and passive shimming technologies. For an accurate mapping of geometrical distortion in 3D, two conditions must be satisfied. First, the number of control points must be sufficiently large to provide a comprehensive mapping of the spatial variation of distortion and second the positional accuracy of these control points must be ensured [1]. In this study, the spatial accuracy of coordinates in 3D space is assessed using a previously reported 3D-printed grid phantom [2] across six clinical MRI scanners at both 1.5T and 3T field strengths. This is achieved by quantifying machine-related MR distortion by comparing the locations of corresponding features in both MR and CT data sets.

Methods

A rigid 170mm×170mm×250mm mesh cuboid insert with a 2mm wireframe was designed, 3D-printed and fixated inside a 240mmφ × 250mm cylinder [2]. Off-the-shelf mineral (baby) oil (Johnson&Johnson, NJ) was used to fill the phantom container to avoid wavelength-induced artefacts [3,4]. Orthographic projections of the 3D model (a,b) and printed insert (c,d) are shown in Fig.1. Each point of intersection between the mesh lines in 3D space is treated as a control point with an approximate spacing of 20.0mm in each dimension. The insert contains a total of 9×9×11 (891) control points. With the axis of the cylinder aligned along the B0 field, MR images were acquired using one Philips (Philips Healthcare, Best, the Netherlands) and five Siemens (Siemens Healthcare, Erlangen, Germany) scanners using the body coil and a 3D gradient-echo sequence. A single k-space line was encoded per TR with a mean acquisition time of 25 minutes per acquisition. Imaging parameters for the 6 clinical MRI scanners are shown in Table1 (Philips [A: Achieva 3T], Siemens [B: Verio 3T, C: Avanto 1.5T, D: Prisma 3T, E: Aera 1.5T, F: Aera 1.5T]). In order to define the true, undistorted

control point positions, a corresponding CT scan of the phantom was generated using a GE LightspeedRT16 system (GE Healthcare, Milwaukee,WI, USA) using a voxel size of 0.71mm×0.71mm in-plane and 1.25mm through-plane.

All of the 891 control points were detected using 3D normalized cross correlation (NCC) using a MATLAB (The Mathworks, Natick, MA) program [2] and were manually inspected. This was achieved by defining two templates of 7×7×7 voxels extracted from the iso-center of the CT and MR acquisitions. We assumed that this point in space was free of distortions in the MR acquisition. Each template was then convolved with its originating volume yielding a volume of correlation coefficients for both the CT and MR acquisitions. Thresholding was then used to determine the control points corresponding to the highest correlating points. Connected components were then computed of the thresholded correlation coefficients and the centroids of each of the control points were determined. A distortion-free distance map was generated from CT. We used the Euclidean distance metric to determine the distance between the two distance maps corresponding to MR and CT control points. The distortion-free distance map was compared to an artificially created volume in MATLAB, which resembled the control point locations in the 3D-printed insert, and a mean error of 0 was found.

Results

Measured distances between the control points in the CT dataset were accurate to within 0.05mm, better than the manufacturer stated value of 0.15mm. Overall mean error across the entire MR volume for each of the 6 scanners employed in this study is shown in Table2. For each of the six scanners, mean error across the volume was less than 2mm. Mean L2-norm errors for the axial and sagittal control point planes is given in Fig.2 (a, b) respectively. Distortion in the central planes for all scanners was less than 2mm. Three scanners (A, C, D) achieved an error of less than 1.6mm across the volume.

Discussion & Conclusions

Detecting spatial accuracy of coordinates in 3D space is essential for determining geometric distortion to aid in MR/CT planning. Design improvements can be made in the 3D-printed insert whereby a larger feature can represent a control point. This will then alleviate the need for manual inspection of the 3D normalized cross correlation, as geometric distortions will often make thresholding of the NCC coefficients difficult. Nevertheless, this is a cost-effective approach to determine the spatial accuracy of control points.

References

[1] Wang et al., A novel phantom and method for comprehensive 3-dimensional measurement and correction of geometric distortion in magnetic resonance imaging, Magnetic Resonance Imaging. (2004), 22, 529-542

[2] Jafar et al., A Regularly Structured 3D Printed Grid Phantom for Quantification of MRI Image Distortion, ISMRM (2015), ePoster 3727

[3] Baldwin et al., Characterization, prediction, and correction of geometric distortion in 3 T MR images, Medical Physics 34(2):388-399

[4] Price et al., Quality Assurance Methods and Phantoms For Magnetic-resonance-imaging - Report of AAPM Nuclear-magnetic-resonance Task Group No-1, Medical Physics 17:287-295

Figures

Fig.1

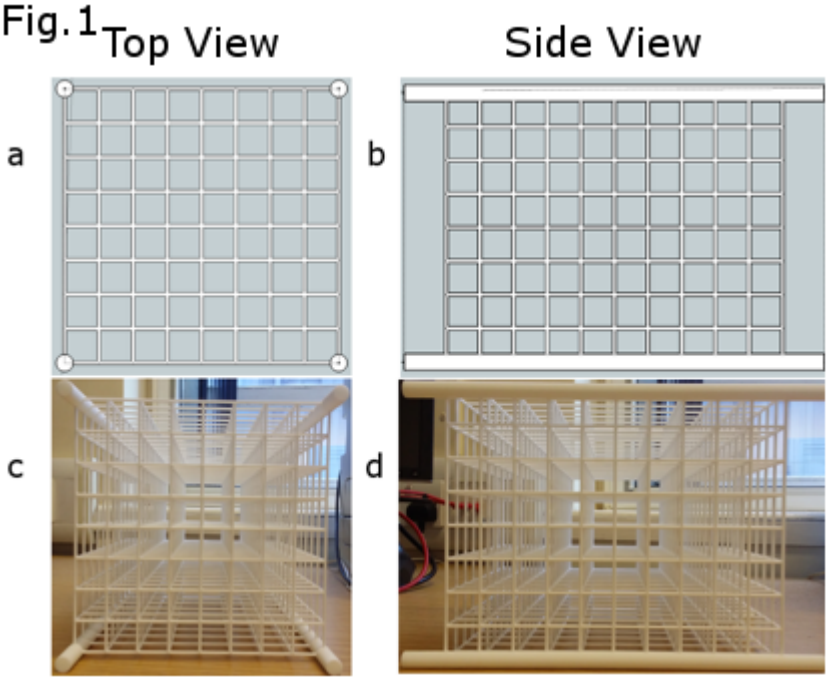

Schematics (a,b) and photographs (c,d) of the 3D printed phantom.

Fig.2

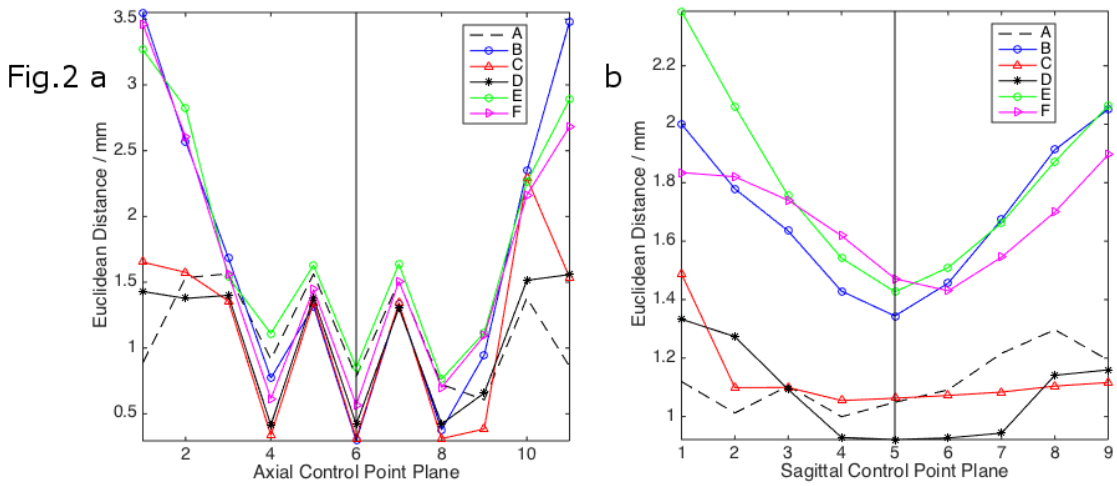

a) Euclidean distance in mm for the Axial and Sagittal control point planes of the phantom. The vertical line in each figure represents the central control point plane in both orientations.

System	TR/TE (ms/ms)	Flip angle (°)	FOV mm × mm	in-plane resolution mm × mm	Slice width (mm)	IF (MHz)
A	11/5.2	30	361 × 361	0.71 × 0.71	1.25	127.7
B	11/5.0	10	256 × 256	1.0 × 1.0	1.0	123.18
C	11/5.2	10	256 × 256	1.0 × 1.0	1.0	63.62
D	11/5.0	30	361 × 361	0.71 × 0.71	1.25	123.25
E	11/5.0	20	361 × 361	0.71 × 0.71	1.25	63.68
F	11/5.0	30	361 × 361	0.71 × 0.71	1.25	63.55

Table1: Imaging parameters for each of the 6 scanners employed in this study (IF = imaging frequency).

System	Mean Error ± std (mm)
A	1.1±0.47
B	1.7±1.3
C	1.1±0.72
D	1.1±0.65
E	1.8±1.1
F	1.7±1.1

Table2: Overall mean error across the entire MR volume for each of the 6 scanners employed in this study.